Structure and spectral-luminescent properties of Er^{3+}:ZnO optical ceramics

Structure and spectral-luminescent properties of Er^{3+}:ZnO optical ceramics

E Gorohova[1,*], L Basyrova[2], I Venevtsev[3], I Alekseeva[1], A Khubetsov[1,], O Dymshits[1], M Baranov[2], M. Tsenter[1], A Zhilin[1], S Eron'ko[1], E Oreschenko[1], P. Rodnyi[3] and P Loiko[4]**

[1] S.I. Vavilov State Optical Institute, 36 Babushkina St., 192171 St. Petersburg, Russia
[2] ITMO University, 49 Kronverkskiy Pr., 197101 St. Petersburg, Russia
[3] Peter the Great St. Petersburg Polytechnic University, 29 Polytechnic str., 195251, St. Petersburg, Russia
[4] Centre de Recherche sur les Ions, les Matériaux et la Photonique (CIMAP), UMR 6252 CEA-CNRS-ENSICAEN, Université de Caen Normandie, 6 Boulevard du Maréchal Juin, 14050 Caen Cedex 4, France

E-mail: *e.gorokhova@rambler.ru, **khubezov@gmail.com

Abstract. Transparent zinc oxide ceramics, undoped and doped with 0.1-2.0 wt% Er^{3+} ions were fabricated by uniaxial hot pressing of commercial oxide powders. The ceramics were characterized by X-ray diffraction, SEM, EDX, Raman, X-ray and optical spectroscopy. The analysis of morphology of Er^{3+}:ZnO ceramics reveals that the main components of texture are hexagonal prism planes similar to those for undoped ceramic. The ZnO grain size decreases with addition of Er_2O_3. The Er^{3+} ions are distributed between the ZnO grains and the Er_2O_3 crystals and do not enter the zinc oxide structure. The luminescence spectra of Er^{3+}:ZnO ceramics contain emission bands originating from the intra-4f shell transitions of Er^{3+} ions and bands assigned to defect states at ZnO. The X-ray luminescence spectra indicate the possible energy-transfer between the ZnO grains and Er^{3+} ions. The defect luminescence band becomes weaker and the X-ray luminescence decay time decreases as the erbium concentration is increased.

1. Introduction

Zinc oxide is widely studied and applied in industry due to its unique properties of wide band gap of 3.37 eV, large exciton binding energy of 60 meV, excellent mechanical–electrical coupling characteristics, high radiation tolerance and low cost [1]. The ZnO performance can be adjusted by means of doping with rare-earth ions. In particular, an addition of Er^{3+} ions may induce a variation of the luminescence properties of ZnO [2] while the 1.54 μm photoemission caused by Er^{3+} intra-4f shell transition can be enhanced due to the ZnO → Er^{3+} energy transfer [3]. In this work, both undoped and Er^{3+}-doped ZnO optical ceramics were prepared. The effect of Er^{3+} concentration on the microstructure, absorption and emission properties of ZnO ceramics were studied.

2. Experimental

The undoped and Er^{3+}-doped ZnO optical ceramics with the Er^{3+} concentration of 0.1-2.0 wt% were fabricated from commercial reagent-grade ZnO and Er_2O_3 powders by uniaxial hot pressing in vacuum at the temperatures of 1150 °C and 1180 °C. The as-sintered ceramic disks were polished to laser-

grade quality from both sides and finally had a diameter of 25 mm and a thickness of ~0.5 mm. The undoped ceramic was pale green coloured. With Er^{3+} doping, the colour changed to rose-grey, Figure 1.

The X-ray powder diffraction (XRD) patterns of ceramics were measured with a Shimadzu XRD-6000 diffractometer, Ni-filtered Cu Kα radiation. The ZnO lattice parameters were determined by Rietveld refinement. The morphology of the polished surface of ceramics was characterized by scanning electron microscopy (SEM) using a MERLIN microscope (Carl Zeiss). The same microscope equipped with an Inca Energy X-Max analyzer was employed for energy dispersive X-ray (EDX) based element mapping. The grain size distribution was analyzed with the ImageJ software.

The Raman spectra were measured with the Renishaw inVia confocal Raman microscope using a Leica ×50 objective (N.A. = 0.75). The excitation wavelength λ_{exc} was 514 nm (an Ar^{+} ion laser). The total transmission spectra in the visible and near-IR were measured using a SPECORD 200 PLUS spectrophotometer. The absorption spectra in the range of 300 – 3300 nm were measured with a Shimadzu UV-3600 spectrophotometer. The spectra of photo-luminescence in the visible were recorded using the same confocal Raman microscope with λ_{exc} = 488 nm. The luminescence at ~1.5 μm was measured using an optical spectrum analyser (AQ6375B, Yokogawa) under excitation by a Ti:Sapphire laser tuned to λ_{exc} = 800 nm. The X-ray luminescence spectra were recorded in the reflection geometry upon continuous excitation by an X-ray tube with a tungsten anode (40 kV, 10 mA). The decay kinetics of X-ray luminescence was recorded using a pulsed X-ray setup with a pulse duration of ~ 1 ns at a voltage of 30 kV and a current amplitude of 500 mA.

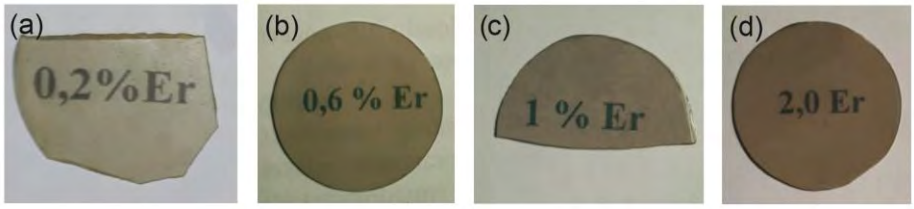

Figure 1(a-d). Photographs of Er^{3+}-doped ZnO transparent ceramics with different Er doping levels: **(a)** 0.2 wt%, **(b)** 0.6 wt%, **(c)** 1.0 wt% and **(d)** 2.0 wt%.

3. Results and discussion

A typical XRD pattern of Er^{3+}-doped ZnO ceramic displaying characteristic wurtzite-type peaks is shown in Figure 2(a). The calculated unit cell parameters for the Er^{3+}-doped ceramics nearly coincide

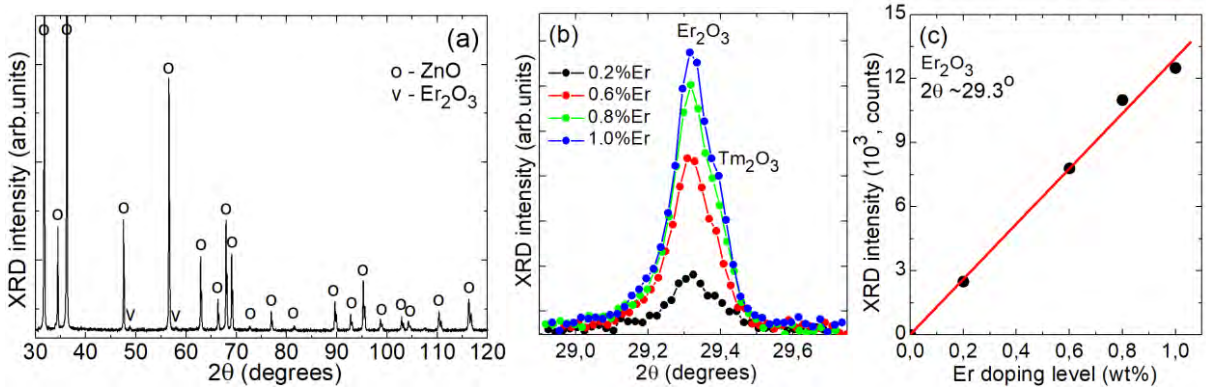

Figure 2(a-c). (a) XRD pattern of 1% Er^{3+} doped ZnO ceramic; **(b)** XRD patterns of ZnO:Er ceramic with different Er doping level in the 2θ range of 28.9 - 29.8° corresponding to the (222) peak of Er_2O_3; **(c)** dependence of the diffraction peak intensity at 2θ ~29.3° on the Er^{3+} concentration. The synthesis temperature is 1150 °C.

with the values obtained for the undoped ZnO (a = 3.249 Å, c = 5.205 Å, ISDD card No 5-0664). It implies that Er^{3+} ions do not enter the ZnO structure. The presence of erbium ions in the form of pure Er_2O_3 in ceramics is evidenced by weak diffraction peaks in the XRD pattern, Figure 2(a), located at diffraction angles 2θ = 49.4° and 58.6° and corresponding to the Miller's indices (*hkl*) = (440) and (622), respectively. The evidence of Er_2O_3 crystallization is manifested by Figure 2(b). The presented fragment of the diffraction pattern for the angles 2θ of 28.9-29.8° contains an unambiguously assigned intense diffraction peak of Er_2O_3 with (*hkl*) = (222) and much weaker side peak due to the possible traces of impurity Tm_2O_3. The diffraction intensity gradually increases with the Er^{3+} doping concentration, Figure 2(c).

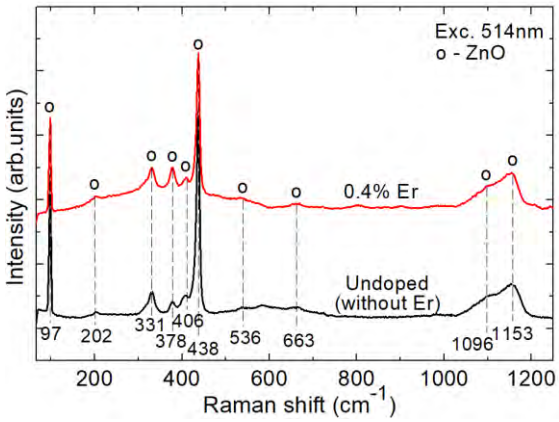

Figure 3. Raman spectra of transparent ceramics: undoped ZnO and 0.4% Er^{3+}-doped ZnO, λ_{exc} = 514 nm. *Numbers* indicate the Raman peak frequencies in cm^{-1}. The curves are shifted for the convenience of observation.

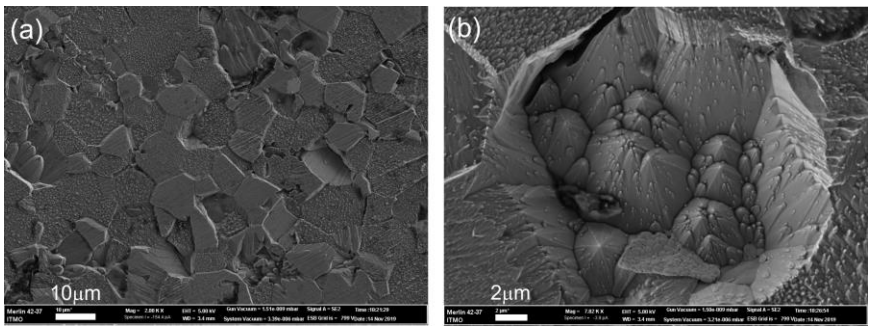

Figure 4(a,b). SEM images of the polished surface of 0.4% Er^{3+}-doped ZnO ceramic. The scale bar is **(a)** 10 μm and **(b)** 2 μm.

Figure 3 shows unpolarized Raman spectra of ZnO optical ceramics, undoped and doped with 0.4 wt% Er. All characteristic wurtzite vibrations are observed in the Raman spectra of both ZnO ceramics at 97, 202, 331, 378, 406, 438, 536, 663, 1096 and 1153 cm^{-1} [4]. A rise in the Raman spectrum of Er^{3+}-doped ceramics in the region of 200–600 cm^{-1} is explained by the contribution of Raman modes of Er_2O_3. The most intense Raman mode of Er_2O_3 appears at ~380 cm^{-1} [5] and overlaps with one of the modes characteristic for ZnO. As a result, the peak at ~378 cm^{-1} is enhanced in the spectrum of Er^{3+}-doped ceramics.

The analysis of the texture of the Er^{3+}-doped ZnO ceramics indicates that that the main components of the texture are the (100) and (110) planes of the hexagonal prism, similar to those for the undoped ceramics. Erbium doping enhances the texture due to the preferred orientation of the prism planes. In the presence of erbium, conditions are created for orientation of the planes of the hexagonal pyramids with gently sloping faces (101), as compared to undoped ceramics.

Data on the nature of the texture of Er^{3+}:ZnO ceramics are consistent with the results of their study by SEM. Numerous grains with smooth facets of the prism and fine-bumpy facets of the negative monohedrons are visible on the surface of the polycrystalline sample, Figure 4(a). Facets of positive monohedrons with characteristic growth microhillocks in the form of hexagonal pyramids, Figure 4(b), are rare. Erbium addition into the ceramics leads to a decrease in the grain size: it ranges from 10 to 35 μm for pure ZnO ceramic and from 5 to 15 μm - for the Er^{3+}-doped ones.

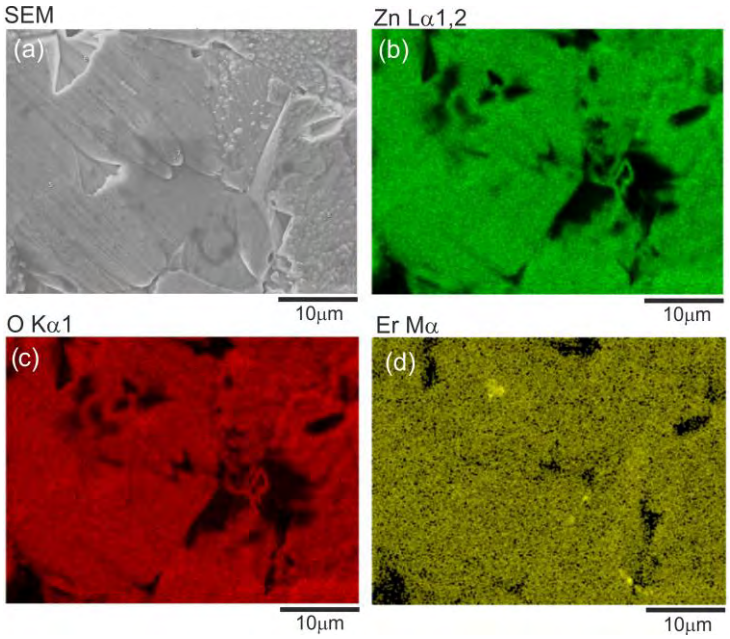

Figure 5(a-d). EDX mapping of 0.4% Er^{3+}-doped ZnO ceramics: **(a)** SEM image, **(b)** zinc mapping (Zn Lα1,2), **(c)** oxygen mapping (O Kα1), and **(d)** erbium mapping (Er Mα).

According to Figure 5, which shows the surface element mapping (Zn, O and Er) for the 0.4 wt% Er^{3+}-doped ZnO ceramics, regions with different microstructures have the same composition. They are formed by zinc, oxygen and erbium uniformly distributed over the sample. There are also irregularly distributed areas enriched in erbium and ranging in size from sub-μm to a few μm. These are probably regions enriched in erbium oxide. These data illustrate the fact that Er^{3+} ions are located at ZnO grain boundaries and form the Er_2O_3 crystals.

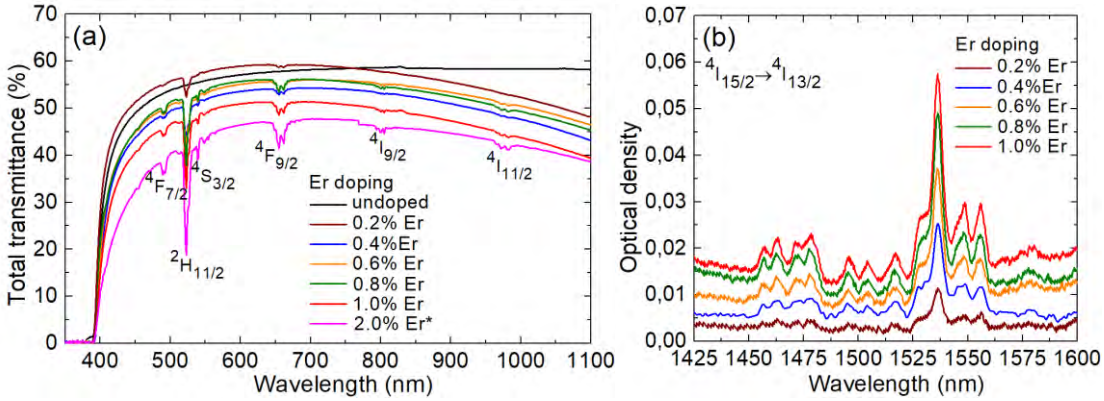

Figure 6(a,b). Optical absorption of Er^{3+}-doped ZnO ceramics: **(a)** total transmittance spectra. *For the sample with 2.0% Er, the synthesis temperature is 1180 °C. **(b)** Absorption band related to the $^4I_{15/2} \rightarrow {}^4I_{13/2}$ Er^{3+} transition; the background scattering losses are subtracted and the spectra are shifted along the vertical axis for their comparison. The sample thickness is ~0.5 mm.

Figure 6(a) shows the transmission spectra of undoped and Er^{3+}-doped ZnO ceramics in the visible and near IR. All doped samples are characterized by a maximum in the transmission curves in the wavelength range 600 - 800 nm. The maximum transmission in the visible varies from ~60% to 45% with the Er content variation from 0.2 wt% up to 2.0 wt%. The UV absorption edge for Er^{3+}-doped samples is about 390 nm. According to the study of transmission spectra in the mid-IR, the limit of the long-wavelength transparency of Er^{3+}:ZnO ceramics shifts from ~4 μm to 2.4-2.5 μm as compared with the spectrum of undoped ceramic. This is a consequence of absorption by free carriers. Their concentration increases from 3.13×10^{18} cm^{-3} (for undoped ZnO) to 8.37×10^{18} cm^{-3} (for Er^{3+}:ZnO).

In the spectra, bands characteristic of Er^{3+} ions are observed at ~489, 522, 538, 654, 802 and 976 nm. They correspond to transitions in absorption from the $^4I_{15/2}$ Er^{3+} ground state to the excited states $^4F_{7/2}$, $^2H_{11/2}$, $^4S_{11/2}$, $^4F_{9/2}$, $^4I_{9/2}$ and $^4I_{11/2}$, respectively. The Er^{3+} absorption spectrum in the region of ~1.5 μm (the $^4I_{15/2} \rightarrow {}^4I_{13/2}$ transition) has a fine structure, Figure 6(b). The shape of Er^{3+} absorption bands for the Er^{3+}:ZnO ceramics well agree with that for the Er_2O_3 oxide [6]. The almost linear dependence of the optical density on the concentration of Er^{3+} ions, Figure 6(b), indicates the implementation of Beer's law, i.e., the distribution of Er^{3+} ions between the crystal interfaces and Er_2O_3 crystals has a constant ratio. The Beer's law is verified for all absorption bands of Er^{3+} ions.

In the photoluminescence spectra upon excitation in the blue, Figure 7(a), structured bands assigned to the intra-4f shell Er^{3+} emissions are observed. Besides that, broad underlying emission at ~500-900 nm with several local maxima at 600, 660 and 770 nm is clearly visible. It is assigned to transitions between various defect states in ZnO, as verified by the study of the undoped ceramics. In contrast, the fingerprint Er^{3+} emission at ~1.5 μm, Figure 7(b), has no underlying background. The intensity of the ~1.5 μm luminescence gradually increases with the erbium content.

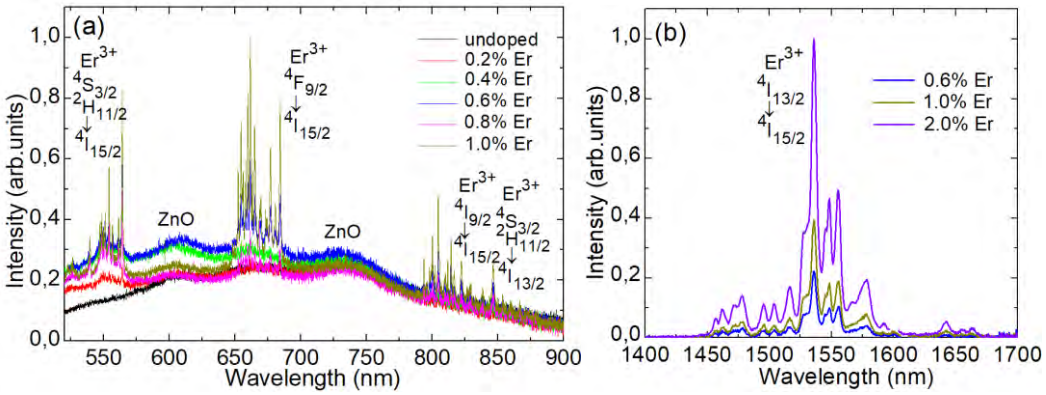

Figure 7(a,b). The spectra of photoluminescence of Er^{3+}-doped ZnO ceramics: **(a)** visible spectral range, λ_{exc} = 488 nm, **(b)** near-IR spectral range, λ_{exc} = 800 nm. In **(a)**, the spectrum for undoped ceramics is given for comparison. For the sample with 2.0% Er, the synthesis temperature is 1180 °C.

X-ray luminescence spectroscopy is a powerful technique to observe the intrinsic and defect-related emissions of ZnO. The measured X-ray luminescence spectra, Figure 8, exhibit two intense emission bands. The first one is centered at ~389 nm and it is due to the near-band-edge (NBE) transitions. The second much broader band is centered at ~514 nm representing the defect state emission. The NBE emission intensity increases with the Er^{3+} content exceeding 0.2 wt%. A significant suppression of the defect band is observed upon adding Er^{3+} into the ceramics.

The average X-ray luminescence decay time in the "fast" time domain of 0–50 ns was 6–8 ns for all the studied Er^{3+}-doped samples and about 65 ns for the undoped ZnO. In the "slow" domain of 50–200 ns, the decay time was 30–40 ns for Er^{3+}-doped samples and 90 ns for the undoped ZnO ceramic.

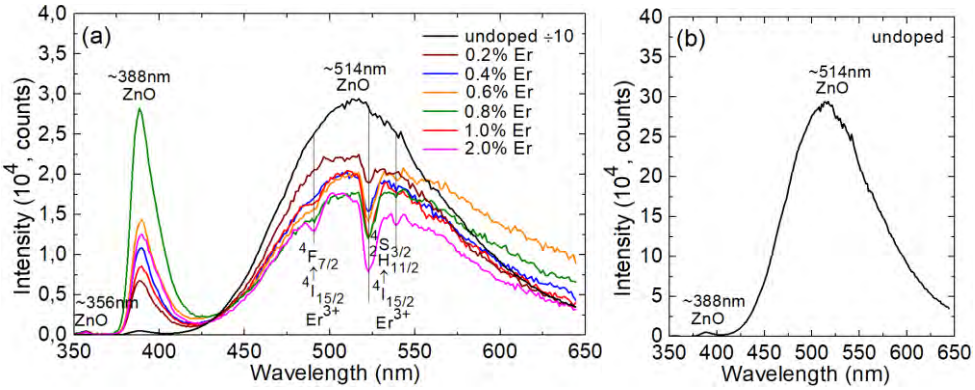

Figure 8(a,b). The spectra of X-ray luminescence of **(a)** Er^{3+}-doped ZnO ceramics **and (b)** undoped ZnO ceramics. In **(a)**, the spectrum for undoped ceramics is divided by a factor of 10. *Vertical lines*: absorption bands of Er^{3+} ions causing deeps in the X-ray luminescence spectra.

4. Conclusions

Erbium ions do not enter the ZnO structure but are located on the ZnO grain surface and form the Er_2O_3 phase at the grain boundaries. The planes of simple forms of Er^{3+}:ZnO grains have all morphological features typical for single crystals. The introduction of Er^{3+} ions enhances the texture inherent for undoped ceramics, but does not change its components. Er doping leads to a reduction of the ZnO grain size. In the Raman spectrum, vibrations characteristic of ZnO crystals are observed. A rise in the Raman spectrum of Er^{3+}-doped ceramics in the region of 200–600 cm^{-1} is explained by the contribution of Raman modes of Er_2O_3.

The absorption spectra of Er^{3+}:ZnO ceramics contain the bands characteristic for Er_2O_3. The validity of the Beer's law is verified indicating the constant distribution of Er^{3+} ions between the surface of ZnO grains and the Er_2O_3 phase. The Er^{3+} doping leads to a significant suppression of the intensity of the green (515-540 nm) ZnO X-ray luminescence band of defective nature, and to an enhancement of the exciton emission at 389 nm. It causes a change in the X-ray luminescence kinetics: the average decay time in the range of 0-50 ns for all Er-doped ceramics decreases by an order of magnitude compared to that for the undoped material. Photoluminescence spectra of ceramics upon excitation at 488 nm and 800 nm exhibit characteristic emission bands of the Er^{3+} ion. The spectral positions of the deeps in the X-ray luminescence spectra coincide with the absorption bands of Er^{3+} ions in Er_2O_3, indicating possible energy-transfer between the excitations to defect states in ZnO grains and Er^{3+} ions in Er_2O_3. The developed Er^{3+}-doped ZnO optical ceramics with transmittance of 40-60% in the visible spectral range possess a high radiation stability. They are promising for optoelectronic applications.

Acknowledgements

This work was partly supported by the RFBR (Grant 19-03-00855).

References

[1] Ozgur U, Alivov Ya I, Liu C, Teke A, Reshnikov M A, Dogan S, Avrutin V, Cho S J and Morkoc H 2005 *J. Appl. Physics* **98** 041301
[2] Loiko P *et al*. 2018 *J. Lumin.* **202** 47
[3] Xiao F, Chen R, Shen Y Q, Dong Z L, Wang H H, Zhang Q Y and Sun H D 2012 *J. Phys. Chem. C* **116**(24) p 13458
[4] Cusco R, Alarcon-Llado E, Ibanez J, Artus L, Jimenez J, Wang B and Callahan M J 2007 *Phys. Rev. B* **75** 165202
[5] Schaack G and Koningstein J A, 1970 *J. Opt. Soc. Am.* **60**(8) 1110
[6] Michael C P *et al*., 2008 *Optics Express* **16** (24) 19649